

**Momentum dependence of superconducting gap, strong-coupling  
dispersion kink, and tightly bound Cooper pairs in the high- $T_c$**

**$(\text{Sr,Ba})_{1-x}(\text{K,Na})_x\text{Fe}_2\text{As}_2$  superconductors**

L. Wray,<sup>1</sup> D. Qian,<sup>1</sup> D. Hsieh,<sup>1</sup> Y. Xia,<sup>1</sup> L. Li,<sup>1</sup> J.G. Checkelsky,<sup>1</sup> A. Pasupathy,<sup>1</sup> K.K. Gomes,<sup>1</sup> C.V. Parker,<sup>1</sup> A.V. Fedorov,<sup>2</sup> G.F. Chen,<sup>3</sup> J.L. Luo,<sup>3</sup> A. Yazdani,<sup>1</sup> N.P. Ong,<sup>1</sup> N.L. Wang,<sup>3</sup> and M.Z. Hasan<sup>1,4,\*</sup>

<sup>1</sup>*Joseph Henry Laboratories of Physics, Department of Physics,  
Princeton University, Princeton, NJ 08544, USA*

<sup>2</sup>*Lawrence Berkeley National Laboratory,  
Advanced Light Source, Berkeley, CA 94305, USA*

<sup>3</sup>*Beijing National Laboratory for Condensed Matter Physics,  
Institute of Physics, Chinese Academy of Sciences, Beijing 100080, P.R. China*

<sup>4</sup>*Princeton Center for Complex Materials,  
Princeton University, Princeton, NJ 08544, USA*

(Dated: 14<sup>th</sup> August, 2008)

## Abstract

We present a systematic angle-resolved photoemission spectroscopic study of the high- $T_c$  superconductor class  $(\text{Sr}/\text{Ba})_{1-x}(\text{K}/\text{Na})_x\text{Fe}_2\text{As}_2$ . By utilizing a photon-energy-modulation contrast and scattering geometry we report the Fermi surface and the momentum dependence of the superconducting gap,  $\Delta(\vec{k})$ . A prominent quasiparticle dispersion kink reflecting strong scattering processes is observed in a binding-energy range of 25-55 meV in the superconducting state, and the coherence length or the extent of the Cooper pair wave function is found to be about 20 Å, which is uncharacteristic of a superconducting phase realized by the BCS-phonon-retardation mechanism. The observed  $40\pm 15$  meV kink likely reflects contributions from the frustrated spin excitations in a  $J_1$ - $J_2$  magnetic background and scattering from the soft phonons. Results taken collectively provide direct clues to the nature of the pairing potential including an internal phase-shift factor in the superconducting order parameter which leads to a Brillouin zone node in a strong-coupling setting.

---

\*To whom correspondence should be addressed: mzhasan@Princeton.EDU

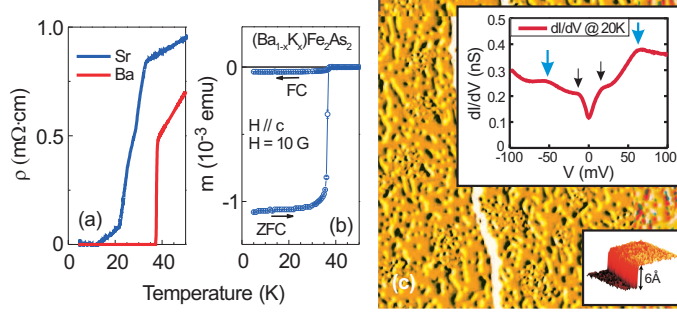


**FIG. 1: Phase transition, magnetization, and STM characterization.** (a-b) Bulk  $T_c$  of crystalline  $(Ba, K)Fe_2As_2$  and  $(Sr, K)Fe_2As_2$  was determined based on the resistivity and magnetization profiles.  $(Ba, K)Fe_2As_2$  samples exhibited  $T_c = 37K$  and  $\delta T_c \sim 1K$  whereas  $(Sr, K)Fe_2As_2$  samples exhibited a broad ( $\sim 10K$ ) transition with a  $T_c \sim 26K$ . (c) Surface quality was studied by atomic-resolution STM which revealed a high degree of flatness and confirmed the suitability for spectroscopic measurements. The derivative of an STM image is shown which was taken on a  $500 \times 500 \text{ \AA}^2$  patch. The inset shows STM data in the superconducting state with a gap of  $2\Delta \approx 30$  meV and kink structures around 40-50 meV loss-energies.

The recent discovery of superconductivity ( $T_c$  up to 55K) in iron-based layered compounds promises a new route to high temperature superconductivity [1, 2, 3]. This is quite remarkable in the view that the  $T_c$  in the pnictides is already larger than that observed in the single-layer cuprates. Preliminary studies suggest that the superconducting state in these materials competes with a magnetically ordered state, and the proper description of the ordered state lies somewhere in between a strong correlation mediated local moment magnetism and quasi-itineracy with stripe-like frustration [3, 4, 5, 6, 7, 8, 9, 10, 11, 12, 13, 14, 15]. This calls for a microscopic investigation of pair formation and related electron dynamics in these superconductors. Angle-resolved photoemission spectroscopy (ARPES) is a powerful tool for investigating the microscopic electronic behavior of layered superconductors [16, 18]. In this work we report electronic structure results focusing on the details of the low-lying quasiparticle dynamics on very high quality ( $\delta T_c \lesssim 1K$  and surface-RMS  $\sim 1 \text{ \AA}$ ) *single domain* single crystal samples, which allow us to gain insight into connections between the superconductivity and magnetism. We observe that the electrons are strongly scattered by collective processes around the 15 to 50 meV binding energy range depending on the Fermi surface sheet while a magnitude-oscillating gap structure persists nearly-along

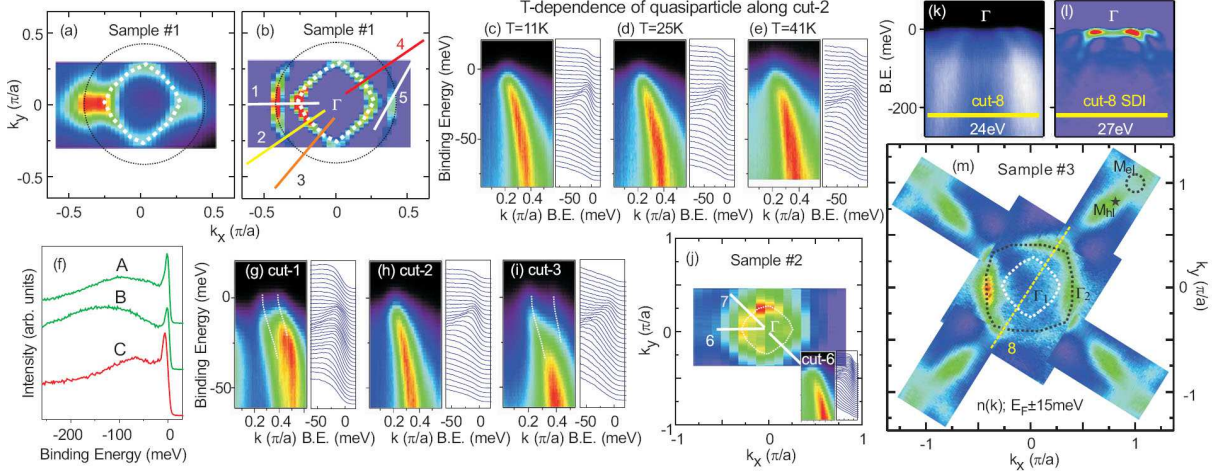


**FIG. 2: Fermi surface and quasiparticle behavior:** (a) ARPES intensity integrated within 15 meV of Fermi level in  $(Ba, K)Fe_2As_2$ . (b) Second-derivative image approximation of the Fermi surface topology around the  $\Gamma$ -point. (c-e) Quasiparticle dispersion along cut-2 and its temperature evolution. (f) High-resolution fine-step binding energy scans shown for some selected k-space points (A, B) near the  $[1,0]$  and  $[1,1]$  axes on the outer FS surrounding the  $\Gamma$  point, and (C) on a separate FS close to the M-point. (g-i) Quasiparticle intensity profiles along k-space cuts 1 to 3. The k-space cut-2 strongly suppresses the outer FS and provides a clear spectroscopic look at the quasiparticle that forms the innermost FS. Because of the spectral clarity this quasiparticle can be studied in quantitative detail. (j) Fermi surface image ( $\pm 15$ meV) taken on  $(Sr, K)Fe_2As_2$ . (k,l) Wide k-range coarse-step scans are shown which were used for locating the Fermi crossings. (m) ARPES intensity map within 15 meV of Fermi energy over the complete BZ measured with a photon energy of 18 eV. Hole- ( $\Gamma_1$ ,  $\Gamma_2$ ,  $M_{hl}$ ) and electron-like ( $M_{el}$ ) Fermi sheets are labeled.

the SDW wave vector of the parent compound. We also show that a Cooper pair in this superconductor is very tightly bound ( $\lesssim 4a_o$ ). Our overall results can be self-consistently interpreted in a phase-shifting order parameter scenario.

ARPES measurements were performed using 18 to 60 eV photons with better than 8 to 15 meV energy resolution respectively and overall angular resolution better than 1% of the Brillouin zone. Most of the data were taken at the Advanced Light Source beamline 12.0.1 and a limited data set was taken at SSRL beamline 5-4, using a Scienta analyzer with chamber pressures lower than  $5 \times 10^{-11}$  torr. Linearly polarized photons were used for all the study. The angle between the  $\vec{E}$ -field of the incident light and the normal direction

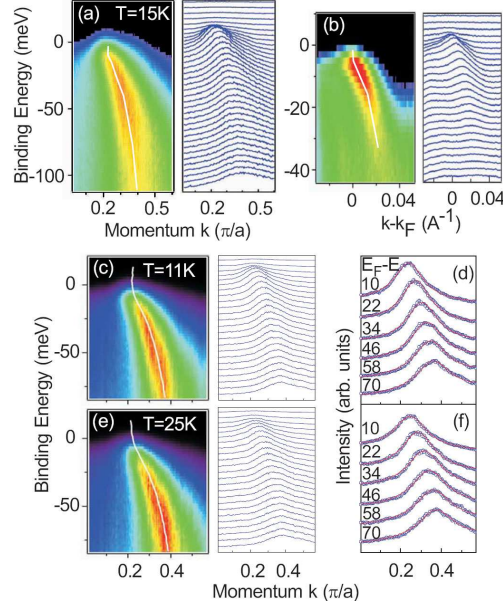


FIG. 3: (a) Quasiparticle band dispersion along cut-4 at 15K. The  $k$ -space cut-4 is approximately along the  $Q_{AF}$ -vector of the undoped compound, as defined in Fig.2(b). (b) Band dispersion for the  $\Gamma_2$  quasiparticle along cut-5 shows a small kink near 18meV. (c,e) Close-up view of dispersion along cut-4 near the 40meV kink at 11K and 25K. The MDCs can be fitted by Lorentzians with linear backgrounds. (d),(f) Quasiparticle lineshapes for panels (c,e) are presented at selected energies (10-70 meV).

of the cleaved surface was set to about 45 degrees (at 12.0.1). Single crystalline samples of  $\text{Ba}_{1-x}\text{K}_x\text{Fe}_2\text{As}_2$  ( $T_c=37\text{K}$ ),  $\text{Sr}_{1-x}\text{K}_x\text{Fe}_2\text{As}_2$  ( $T_c=26\text{K}$ ) and  $\text{Sr}_{1-x}\text{Na}_x\text{Fe}_2\text{As}_2$  ( $T_c=36\text{K}$ ) were used for this systematic and class-independent study of the kink phenomena. Cleaving the samples in situ at 15K resulted in shiny flat surfaces. Cleavage properties were thoroughly studied and characterized by atomic resolution STM measurements and the surface was found to be flat, with an RMS deviation of  $1\text{\AA}$ (Fig.1(c)) and rarely observed steps of size  $6\text{\AA}$ . Sample batches with  $\delta T_c \sim 1\text{K}$  and smooth STM images were selected for UHV cleaves in the ARPES studies here. The utilization of unique scattering geometries coupling with specific photon energy contrasts ( $18\pm 2\text{ eV}$  vs.  $40\pm 2\text{ eV}$ ) allowed us to selectively suppress one of the FS sheets so that the other can be studied in details.

Quasiparticle behavior around the  $\Gamma$ -FS sheets is shown in Figure 2. Two square-like FS sheets were clearly resolved near the center of the BZ, labeled  $\Gamma_1$  and  $\Gamma_2$  in Fig.2(m). An azimuthal variation of ARPES intensity around the FS pockets was observed, and found to

be most pronounced at 40eV incident energy for the scattering geometry described above. A comparison of quasiparticle dispersion measured along the various  $\vec{k}$ -space cuts suggests that looking roughly along the cuts 30 to 40-degrees to the  $\Gamma$  to  $(\pi, 0)$ -line provides a clear spectroscopic view of the quasiparticle dispersion and lineshape behavior on the inner-FS. This is also the cut that is nearly parallel to the SDW vector (undoped compound). A bend in dispersion could be observed in the cut-2 data which is not resolved in cut-1 or 3 data due to the spectral overlap with the outer-FS (two bands).

A closer look at the quasiparticle dispersion behavior is presented in Figure 3. A bend in dispersion is evident in the momentum distribution curves (MDC) taken on a crossing near the  $\Gamma_1$ -FS (cut-4). Each MDC could be fitted with a single Lorentzian over a wide binding energy range and, as in the raw data sets, the fitted peak positions trace a kink around  $40 \pm 15$  meV. This is further seen by examining the peak position of the real part of the self-energy (Fig.4). Although it is less clear, the MDC width plotted as a function of the electron binding energy is found to exhibit a drop below 35 meV which is consistent with a kink in a nearby binding energy as seen in the raw data. At temperatures above  $T_c$  the kink shifts to somewhat lower energies. As the temperature is raised further the MDCs are broadened making its identification or analytic extraction from our experimental data difficult. In the MDC widths an increase is observed at very low energies which is due to some residual signal from the tail of the quasiparticles from the outer FS. Our STM data in Fig.1(c) also exhibit a satellite structure around 40-50 meV loss-energy range (with respect to the quasiparticle peak position) consistent with the observed ARPES kink. Assuming that the kink reflects coupling to some bosonic-like modes one can estimate the coupling strength:  $\lambda'_{eff} \gtrsim (0.7/0.45 - 1) \sim 0.6$ . This coupling is about a factor of two to three larger than the electron-phonon coupling ( $\lambda_{ph} \sim 0.2$ ) calculated for the Fe-As phonons near 20-40 meV [5, 6]. A careful look at the outer central FS ( $\Gamma_2$  band, cut-5) also reveals a kink around  $18 \pm 5$  meV. This kink is revealed when the band associated with the inner-FS sheet is suppressed by a choice of incident photon energy (18 eV).

If the kink phenomenon is intimately related to the pairing potential one might expect some inter-correlation between the kink energies and the superconducting gaps at different FS sheets. In order to investigate this aspect we present the gap evolution data taken in these kink-exhibiting samples in Figure 5. The opening of the superconducting gap is viewed upon symmetrization (see Ref-[17] for methods) and a gap magnitude of about  $13 \pm 2$  meV is

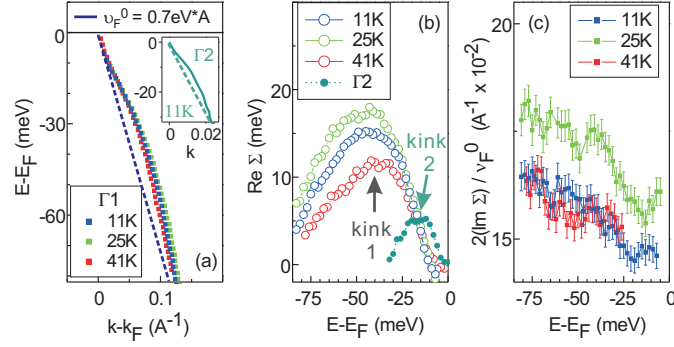


FIG. 4: (a) By tracing the peak positions, quasiparticle band dispersion is plotted at  $T=11\text{K}$ ,  $25\text{K}$  and  $41\text{K}$ . At all temperatures, the dispersion curve shows a “kink”-like feature at  $40\pm 10\text{ meV}$ . The gray dashed line illustrates the “bare” band used for the self-energy estimation. The smaller kink at  $18\pm 5\text{ meV}$  on the  $\Gamma_2$  band is shown in the inset. (b) The real part of self energy is obtained by subtracting the gray dashed line from the experimental band dispersion. Peak position is used to define the “kink” position. (c) Fitted MDC width as a function of binding energy for quasiparticles on  $\Gamma_1$ . A small offset in the  $T=25\text{K}$  intrinsic width is due to temperature dependent shifting of beam position on the sample.

quite evident at low temperatures, in agreement with ref. [19]. This value is consistent with the spatially-averaged gap ( $< 15\text{ meV}$ ) we have obtained with STM (see Fig.1(c)) on the same batch of samples and these observations (ARPES in Fig.5 and STM in Fig.1) confirm that the kinks survive the superconducting gap formation. Although our FS topology and an intrinsic fluctuation regime differs from that in Ref-[18]. Evidently, a more complex gap and a different FS topology (M-pockets) have been realized in our  $(Ba/Sr, K/Na)Fe_2As_2$  series than that in the NdFeAsO series [18]. The fine details here, made possible via selective study of the bands, allow us to look for correlations between the gap and the kink. The observed kink energies do (Fig.3) seem to scale ( $40\text{ meV}$  and  $18\text{ meV}$ ) with the superconducting gap energies ( $13\text{ meV}$  and  $6\text{ meV}$ ) on the two central Fermi surfaces (Fig.4). The coupled cross-sections of bands near the M-point ( $M_{hl}$  and  $M_{cl}$  in Fig.2(m)) for modulated incident photon energy make a systematic study of kinks in that region of momentum space difficult. We note that our particular gap structure is consistent with an order-parameter that takes, qualitatively, the form of  $\Delta_o \cos(k_x) \cos(k_y)$  within the plane (see fit in Fig.5(e)). Although fine details of the gap anisotropy are not resolved due to lack of resolution, the

gap on the  $\Gamma_2$  FS is smaller than the  $\Gamma_1$  gap by a  $\cos(k_x)\cos(k_y)$  factor, e.g. along the  $\hat{x}$  axis:  $\cos(.40\pi/\sqrt{2})^2/\cos(.27\pi/\sqrt{2})^2=.58\sim\Delta(\Gamma_2)/\Delta(\Gamma_1)=7\text{meV}/14\text{meV}$ . The large gap ratio,  $\frac{2\Delta}{k_B T_c}=8$  for the innermost gap of 13meV, is a clear sign of strong coupling. The systematic oscillation pattern and FS topology in our data suggest that the “node” of the  $\cos\times\cos$  order parameter lies in between the  $\Gamma_2$  band and the corner pockets, but it clearly lies outside (Fig.5) the Fermi contour. Yet, we caution that our ARPES data do not rule out the possibility of an out-of-plane ( $k_z$ ) node in the order parameter, therefore the case for completely nodeless superconductivity remains open. Existence of such a node may explain the in-gap  $T^3$  behavior of NMR data [20], and could potentially be established by mapping the ARPES gap distribution over a wide range of incident energies.

A strong-coupling kink phenomenology is observed in the electron dynamics of high  $T_c$  cuprates which occurs around  $60\pm 20$  meV, as observed by ARPES and STM, and is often attributed to phonons or magnetism or polarons with  $\lambda'_{eff}\sim 1$  to 1.5 [16]. In cuprates the superexchange coupling is on the order of 130 meV, whereas the optical phonons are in the range of 40 to 80 meV overlapping with the kink energy. In the pnictides, although a  $T_c$  value of 37K is not outside the phonon-induced strong-coupling pairing regime, the vibrational modes of the the FeAs plane are rather soft ( $\leq 35$  meV) making electron-phonon interaction [5, 6] an unlikely source of the major part of the quasiparticle’s self-energy beyond 40 meV, considering the observed coupling  $\lambda'_{eff}\gtrsim 0.6$  for the FeAs compounds. The parent compounds of superconducting FeAs exhibit a robust SDW groundstate [3] due to a  $\vec{Q}=(\pi, \pi)$  inter-band instability or due to the interaction of quasi-localized moments and the short range SDW order seems to survive well into the superconducting doping regime [21]. The doping evolution of the Fermi surface lacks robust nesting conditions for purely band-magnetism to be operative at these *high dopings* and the relevant magnetism here likely comes from the local exchange energy scales in a doping induced frustrated background. Therefore, quite naturally, strong spin fluctuations in the presence of electron-electron interaction are important contributors to the self-energy at high dopings. In accounting for the parent SDW groundstates of these materials the known values of  $J_1$  and  $J_2$  are on the order of 20 to 50 meV [13, 14]. In an itinerant picture, there exists a Stoner continuum whose energy scales are parameterized by the exchanges whereas in a local picture,  $J_1$  and  $J_2$  reflect Fe-Fe and Fe-As-Fe superexchange paths and the groundstate is a highly frustrated doped Heisenberg magnet [14]. The proper description of the experimentally observed magnetism



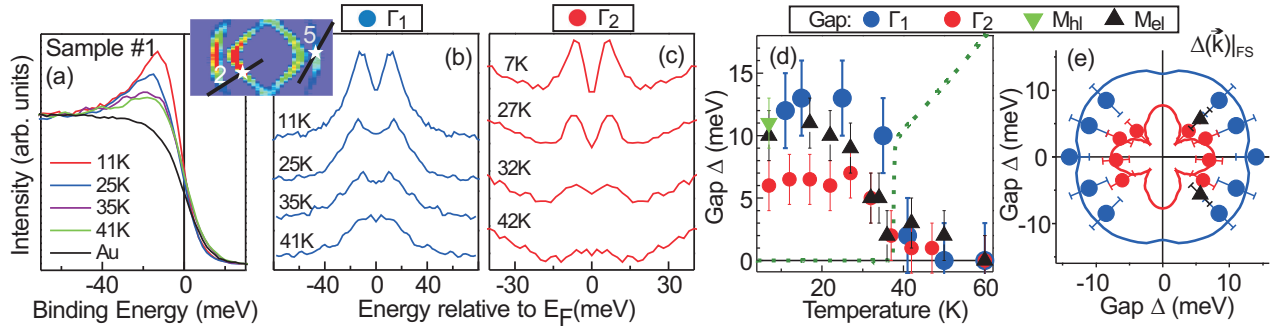


FIG. 5: **Momentum and Fermi-surface dependence of superconducting gap:** (a) temperature dependence of quasiparticles (cut-2) near the Fermi level through the superconducting transition. Below  $T_c$  samples exhibit coherence-peak-like behavior similar to what is observed in some cuprates. Temperature dependence of the gap at the k-space location of (b) the inner-most ( $\Gamma_1$ ) FS and (c) the outer central ( $\Gamma_2$ ) FS are estimated by symmetrization around  $E_F$ . (d) The temperature dependence of the gaps measured at different FS locations ( $\Gamma_1$ -FS, blue;  $\Gamma_2$ -FS, red;  $M_{hl}$ , green;  $M_{el}$ , black) are plotted along with the bulk resistivity curve (dotted green). A fluctuation regime above  $T_c$  is observed. (e) The azimuthal k-dependence of gaps,  $\Delta(k)$ , are shown for different FS sheet locations on a polar plot. Blue and Red solid lines are contours of the  $\cos \times \cos$  function for the Fermi surface outlined in Fig.2(m).

lies somewhere in between. In our photoemission process, removal of an electron from the crystal excites the modes the electron is coupled to, so the observed quasiparticle breaks the locally frustrated magnetic bonds (near-neighbor spin correlation) associated with energy-costs parameterized by  $J_1$  and  $J_2$  which then contributes an energy scale on the order of  $(J_1 + 2J_2)/2 \lesssim 50$  meV in the self-energy of the *doped* system. Since this scale is large it is expected that our 40 meV kink would survive above  $T_c$  which is consistent with our observation. Despite the high signal-to-noise quality of our data, it is difficult to draw an intimate connection or relation [kink(18 meV)  $\approx$  gap(6 meV) + spin-mode(14 meV)] between the low-energy kink and spin-mode (e.g. magnon) [22] without a full phase-diagram study.

Our high-resolution (Fig.3) measurements allow us to estimate the Fermi velocity of the normal state to be about  $0.7 \text{ eV} \cdot \text{\AA}$ . Using the observed superconducting gap (ARPES or STM data in Fig.1) we can estimate the average size of the Cooper pair wavefunction  $\xi = \frac{\hbar v_F}{\pi \Delta}$  by invoking the uncertainty relation [23]. Taking average  $v_F$  (Fig.3 and 2)  $\sim 0.7 \pm 0.1 \text{ eV} \cdot \text{\AA}$

and a gap (Fig.4) value of  $\Delta \sim 13 \pm 2$  meV, this gives  $\xi \lesssim 20 \text{ \AA}$ . This value is remarkably consistent with the high magnitude of  $H_{c2}$  ( $\sim 70\text{T}$ ) [24] reported in these same materials. The ARPES based Cooper pair scale and unusually high  $H_{c2}$  clearly suggest that the Cooper pairs in this class of FeAs superconductors are tightly bound which is in contrast to the point-contact Andreev spectroscopy results on Sm-based FeAs superconductors exhibiting a conventional BCS ratio [25]. The agreement between ARPES, bulk  $H_{c2}$  and the bulk resistivity profile (Fig.5(d)) provides further support for our identification of the superconducting gap and its bulk-representative value through our surface-sensitive measurements (STM and ARPES) here. This also confirms that the ARPES gaps are not the SDW gaps as theoretically claimed by some authors. More importantly, such a small Cooper pair size scale ( $\sim 4a_o$ ) is not known in any phonon-based BCS superconductor [26] but has only been observed in unconventional strongly correlated superconductors. Our observed value is much smaller than that in the s-wave BCS-phonon superconductors such as  $\text{MgB}_2$  [26]. In fact, a combination of small Cooper pair size, oscillating but in-plane nodeless gap function is qualitatively consistent with an unconventional  $\Delta_o \cos(k_x) \cos(k_y)$  (in the unfolded BZ with one iron atom per unit cell)-type or  $s_{x^2y^2}$  or  $s_{\pm}$  wave states [6, 7, 8, 9, 10, 11, 12] since such an order parameter (its Fourier transform) has a nearest-neighbor (NN) or next-NN structure in real space and thus a reduction of the Coulomb interaction within the pair is naturally possible, so the electrons can come closer to each other leading to a short coherence scale. In cuprates, pairing electrons come close to each other, and the short coherence length is achieved by introducing a node in the order parameter ( $d$ -wave) leading to a reduction of Coulomb interaction within the pair. This is often the only choice in a single band correlated system (cuprates or organics). In pnictides, multiband structure can accommodate a phase change without the need for introducing a “node” [27] on the FS, therefore an isotropic gap and a short pairing scale can co-exist with a phase shifted order-parameter structure with a BZ node. Our data suggest that the BZ node lies in between the  $\Gamma_2$  and the corner FS locations along the magnetic wave vector. Our data also suggest that at higher dopings, (possibly beyond  $x=0.4$ ), this BZ node will intersect the sample FS and a *nodal* superconducting state will be realized. While the observation of the strong-coupling kink ( $\sim 40$  meV) is an important first step, its detailed quantitative interpretation will require complete phase diagram study once single-crystals become available also at higher dopings.

In summary, we have presented a Fermi surface and momentum dependence of the super-

conducting gap study of high- $T_c$  superconductor class  $(\text{Sr}/\text{Ba})_{1-x}\text{K}_x\text{Fe}_2\text{As}_2$ . Our systematic spectroscopic data suggest an unusually small dimension of the Cooper pair, kink phenomena (seen both in ARPES and STM around 40 meV in our data here), and an oscillating gap function, all of which collectively point to an unconventional pairing potential. We have presented arguments that in the presence of magnetism, the observed short pairing scale and a nearly-isotropic in-plane gap can be self-consistently realized if the order parameter contains a non-trivial internal  $\pi$  phase-shift factor.

- 
- [1] Y. Kamihara, T. Watanabe, M. Hirano, and H. Hosono, *J. Am. Chem. Soc.* **130**, 3296 (2008); Z.A. Ren, W. Lu, J. Yang, W. Yi, X.L. Shen, Z.C. Li, G.C. Che, X.L. Dong, L.L. Sun, F. Zhou, Z.X. Zhao, *Chin. Phys. Lett.* **25**, 2215 (2008).
- [2] G. F. Chen, Z. Li, D. Wu, G. Li, W. Z. Hu, J. Dong, P. Zheng, J. L. Luo, N. L. Wang, *Phys. Rev. Lett.* **100**, 247002 (2008); X. H. Chen, T. Wu, G. Wu, R. H. Liu, H. Chen, D. F. Fang, *Nature* **453**, 761 (2008).
- [3] C. de la Cruz, Q. Huang, J. W. Lynn, Jiying Li, W. Ratcliff II, J. L. Zarestky, H. A. Mook, G. F. Chen, J. L. Luo, N. L. Wang, P.C. Dai, *Nature* **453**, 899 (2008).
- [4] D.J. Singh and M.H. Du, *Phys. Rev. Lett.* **100**, 237003 (2008).
- [5] L. Boeri, O. V. Dolgov, and A. A. Golubov, *Phys. Rev. Lett.* **101**, 026403 (2008).
- [6] K. Haule, J. Shim and G. Kotliar, *Phys. Rev. Lett.* **100**, 226402 (2008).
- [7] K. Kuroki, S. Onari, R. Arita, H. Usui, Y. Tanaka, H. Kontani, H. Aoki, *Phys. Rev. Lett.* **101**, 087004 (2008)
- [8] I.I. Mazin, D.J. Singh, M.D. Johannes, M.H. Du, *Phys. Rev. Lett.*, **101**, 057003 (2008).
- [9] Z.-J. Yao, J.-X. Li and Z.D. Wang arXiv:0804.4166v2 (2008).
- [10] K. Seo, B.A. Bernevig and J.P. Hu arXiv:0805.2958 (2008).
- [11] M. Korshunov and I. Eremin arXiv:0804.1793v1 (2008).
- [12] V. Cvetkovic and Z. Tesanovic arXiv:0804.4678v3 (2008).
- [13] T. Yildirim, *Phys. Rev. Lett.* **101**, 057010 (2008); Q. Si and E. Abrahams *Phys. Rev. Lett.* **101**, 076401 (2008).
- [14] F. Ma, Z.-Y. Lu and T. Xiang, arXiv:0806.3526 (2008).
- [15] C. Fang, H. Yao, W.F. Tsai, J.P. Hu, S. A. Kivelson, *Phys. Rev. B* **77**, 224509 (2008).

- [16] A. Damascelli, Z. Hussain, Z.X. Shen, *Rev. Mod. Phys.*, **75**, 473(2003); J. C. Campuzano, M. R. Norman and M. Randeria, Photoemission in the high  $T_c$  superconductors, v-2, p167265. Springer, Berlin, (2004); P.D. Johnson *et.al.*, *Phys. Rev. Lett.* **87**, 177007 (2001); P. V. Bogdanov, A. Lanzara, S. A. Kellar, X. J. Zhou, E. D. Lu, W. J. Zheng, G. Gu, J.-I. Shimoyama, K. Kishio, H. Ikeda, R. Yoshizaki, Z. Hussain, Z. X. Shen, *Phys. Rev. Lett.* **85**, 2581 (2000).
- [17] M.R. Norman, M. Randeria, H. Ding and J. C. Campuzano, *Phys. Rev. B* **57**, R11093 (1998).
- [18] C. Liu, T. Kondo, M. Tillman, M. Tillman, G. D. Samolyuk, Y. Lee, C. Martin, J. L. McChesney, S. Bud'ko, M. Tanatar, E. Rotenberg, P. Canfield, R. Prozorov, B. Harmon, A. Kaminski, arXiv:0806.2147v1 (2008).
- [19] H. Ding, P. Richard, K. Nakayama, T. Sugawara, T. Arakane, Y. Sekiba, A. Takayama, S. Souma, T. Sato, T. Takahashi, Z. Wang, X. Dai, Z. Fang, G. F. Chen, J. L. Luo, N. L. Wang, *Europhys. Lett.* **83**, 47001 (2008).
- [20] H.-J. Grafe, D. Paar, G. Lang, N. J. Curro, G. Behr, J. Werner, J. Hamann-Borrero, C. Hess, N. Leps, R. Klingeler, B. Behner, *Phys. Rev. Lett.* **101**, 047003 (2008).
- [21] H. Chen, Y. Ren, Y. Qiu, W. Bao, R. H. Liu, G. Wu, T. Wu, Y. L. Xie, X. F. Wang, Q. Huang, X. H. Chen, arXiv:0807.3950v1 (2008).
- [22] A. D. Christianson, E. A. Goremychkin, R. Osborn, S. Rosenkranz, M. D. Lumsden, C. D. Malliakas, I. S. Todorov, H. Claus, D. Y. Chung, M. G. Kanatzidis, R. I. Bewley, T. Guidi, arXiv:0807.3932v1 (2008).
- [23] M. Tinkham, "Introduction to Superconductivity", 2nd Ed., McGraw-Hill, New York (1996).
- [24] H. Q. Yuan, J. Singleton, F. F. Balakirev, G. F. Chen, J. L. Luo, N. L. Wang, arXiv:0807.3137v2 (2008).
- [25] T. Y. Chen, Z. Tesanovic, R. H. Liu, X. H. Chen, C. L. Chien, *Nature* **453**, 1224 (2008).
- [26] E. W. Carlson, V. J. Emery, S. A. Kivelson, and D. Orgad, in *The Physics of Conventional and Unconventional Superconductors*, edited by K. Bennemann and J. Ketterson (Springer-Verlag, Berlin, 2002).
- [27] The  $\cos \times \cos$  or  $s_{\pm}$  gap does have a node in it but the node does not intersect the Fermi surface as we measure here (Figure 4). However, it is clear that nearest or next nearest neighbour structure of the gap lowers the kinetic energy as opposed to a constant on-site s-wave gap.